THESIS

INVESTIGATING THE IMPACT OF FORCED AND INTERNAL CLIMATE VARIABILITY ON FUTURE CONVECTIVE STORM ENVIRONMENTS IN SUBTROPICAL SOUTH AMERICA: A LARGE ENSEMBLE APPROACH

Submitted by

Anindita Chakraborty

Department of Atmospheric Science

In partial fulfillment of the requirements

For the Degree of Master of Science

Colorado State University

Fort Collins, Colorado

Summer 2023

Master's Committee:

Advisor: Kristen Rasmussen
Co-Advisor: James Hurrell

Brooke Anderson

ABSTRACT

INVESTIGATING THE IMPACT OF FORCED AND INTERNAL CLIMATE VARIABILITY ON FUTURE CONVECTIVE STORM ENVIRONMENTS IN SUBTROPICAL SOUTH AMERICA: A LARGE ENSEMBLE APPROACH

Subtropical South America (SSA) has some of the most intense deep convection in the world. Large hail and frequent lightning are just two of the hazards that profoundly affect people, agriculture, and infrastructure in this region. Therefore, it is important to understand the future convective storm environments over SSA associated with climate change and how these large-scale environmental changes are likely to change high-impact weather events in the future. Previous studies have used convection-permitting regional models and radar data to examine convective storm environments in the current climate across different regions of South America. Here, we use a large ensemble of Earth system model simulations to quantify anthropogenically-driven future changes in large-scale convective environments, as well as how those forced changes might be modified by unforced, internal climate variability. Specifically, we examine changes in different thermodynamic parameters of relevance to severe weather events over SSA in austral spring and summer (September-February). We use daily data from a 50-member ensemble from 1870-2100 performed with version two of the Community Earth System Model (CESM2). Results indicate that no forced changes in convective environments are evident until very late in the 20th century. However, increases in convective available potential energy and atmospheric stability, as well as an increase in lower tropospheric vertical wind shear, became apparent around 1990, and these trends are projected to continue throughout the rest of this

century. The implication is that future large-scale environments may be favorable for less frequent, but perhaps more intense and severe convective modes and their associated hazards. Results also demonstrate that anthropogenic changes are likely to be significantly modified, regionally, by internal climate variability.

ACKNOWLEDGEMENTS

I would like to express my deepest gratitude and appreciation to several individuals who have played a crucial role in the completion of this thesis.

First and foremost, I am immensely grateful to my supervisors, Dr. James Hurrell and Dr. Kristen Rasmussen. Their invaluable guidance, unwavering support, and expert knowledge have been instrumental in shaping this research. Their commitment to academic excellence, insightful feedback, and patience throughout the entire process have been truly exceptional. I am truly fortunate to have had the opportunity to work under their mentorship. I would also like to express my sincere appreciation to Dr. Lantao Sun for his valuable contributions and support. Additionally, I would like to extend my appreciation to my thesis committee, Dr. Brooke Anderson for her invaluable feedback and constructive criticism that have undoubtedly enhanced the quality and depth of this work.

I would also like to extend my heartfelt thanks to my loving husband, whose unwavering support and encouragement have been an immense source of strength for me. His understanding, patience, and belief in my abilities have been unwavering, even during the most challenging times. Without his constant love and support, this journey would not have been possible.

Lastly, I would like to acknowledge the contributions of my colleagues and friends who have provided valuable insights and feedback throughout my research. Their input and discussions have greatly enriched my understanding and have helped shape the outcome of this thesis.

DEDICATION

This thesis is dedicated to my parents, who have always encouraged my passion for science.

TABLE OF CONTENTS

ABSTRACT …….. ii

ACKNOWLEDGEMENTS …….. iv

DEDICATION ……... v

LIST OF FIGURES ……..... vii

Chapter 1 Introduction ……...……..... 1

Chapter 2 Methodology ……...…….. 5

2.1 Data and Model Simulation……..... 5

2.2 Parameters ……..……..……6

2.2.1 Convective Available Potential Energy (CAPE) ……. 6

2.2.2 Convective Initiation (CIN) ……. 7

2.2.3 Tropospheric Wind Shear …… 7

2.2.4 CAPES06 ……. 8

2.3 Model verification …….. 8

Chapter 3 Results and Discussions ……...……... 13

3.1 Ensemble Mean (Forced change) Results over South America ……... 13

3.2 Forced Changes over Subtropical South America ……. 18

3.3 Internal Climate Variability …… . 19

Chapter 4 Conclusions ……..…….. 24

References …… 26

LIST OF FIGURES

Figure 1: Region of interest in the study ……6

Figure 2: ERA5 and CESM2-LE climatology of CAPE ……9

Figure 3: Regression of CAPE onto the ENSO 3.4 index for ERA5 and CESM2-LE……..10

Figure 4: Regression of convective indices area averaged of SSA onto global SST……12

Figure 5: Regression of SSA CAPE onto global SST for CESM2-LE and ERA5 ……...12

Figure 6: Time series of convective indices from 1870-2100 ……..14

Figure 7: Seasonal linear trend of CAPE……...15

Figure 8: Seasonal linear trend of CIN……..15

Figure 9: Seasonal linear trend of S06……...17

Figure 10: Seasonal linear trend of CAPES06……...17

Figure 11: Time series of Austral spring and summer SSA from 1870-2100……..……18

Figure 12: Histogram of linear trend of convective indices……..20

Figure 13: Spatial patterns of forced and internal variability of CAPE……22

Figure 14: Spatial patterns of forced and internal variability of CIN……23

Figure 15: Spatial patterns of forced and internal variability of S06……23

Chapter 1 Introduction

Severe convective storms pose a substantial threat to communities, agriculture, and infrastructure around the world. Each year hazards associated with severe weather cause damages that amount to billions of dollars (Taszarek et al., 2021). Therefore, it is important to understand how the large-scale thermodynamic and kinematic environments that are conducive to severe weather are likely to be influenced by anthropogenic climate change. Most research on this topic has centered on severe weather across the United States. Less attention has focused on other regions, including South America (SA), a region with a broad range of topography, ecosystems, urban and rural territories, cultures, and climates. The majority of SA countries are highly vulnerable to climate change and possess low adaptive capacities (IPCC, 2022). In addition, SA has some of the world's most extreme deep convective cloud systems (Zipser et al., 2006; Romatschke & Houze, 2010; Houze et al., 2015). It is also well known that rainfall from thunderstorms and mesoscale convective systems (MCS) play a significant role in influencing agricultural and socioeconomic conditions in SA (Rasmussen et al., 2016). Therefore, it is important to understand how the convective environment of this region is likely to change with increasing concentrations of greenhouse gases in the atmosphere.

The climate of SA is influenced by the Andes, one of the largest mountain ranges in the world. It creates mesoscale and synoptic-scale phenomena, resulting in divergent climate conditions on the eastern and western slopes and nearby lowlands (Garreaud, 2009). The Andes block zonal flow and, thus, impact regional wind patterns and precipitation. They are also crucial to the development of the South American low-level jet (SALLJ) (Campetella & Vera, 2002). As low-level trade winds from the equatorial Atlantic are blocked and deflected, a barrier jet flows

along the eastern flanks of the Andes (Virji, 1981) and transports moisture to subtropical regions of the continent from the Amazon (Vera et al., 2006). Because of the extreme vertical extent of the Andes, South American storms tend to be closely associated with topography during the process of upscale organization and development related to enhanced lee cyclogenesis and flow modification (Rasmussen & Houze, 2011, 2016).

Within the South American continent, Subtropical South America (SSA) has the deepest and most intense storms (Zipser et al., 2006; Rasmussen & Houze, 2011; Houze et al., 2015) because of the flux of warm and moist low-level air from the Amazon basin transported by the SALLJ (Vera et al., 2006; Insel et al., 2010; Montini et al., 2019). The lee side subsidence of mid-level dry air associated with the westerlies flows over the Andes and creates an elevated mixed layer (Ribeiro and Bosart, 2018) that often acts as a capping inversion for the low-level moist air. This allows the large-scale environment to build up instability to extremely high levels, which leads to extreme deep convection (Rasmussen & Houze, 2011). During the austral summer season, the storms shift southwestward toward the foothills of the Andes where mesoscale convective systems develop and spread eastward (Rasmussen et al., 2014).

One way to understand how the large-scale convective environment might change in the future is through the examination of convective parameters, such as Convective Available Potential Energy (CAPE) and Convective Inhibition (CIN). CAPE measures the energy available for vertical motion in a storm environment, whereas (CIN) represents the stability of the boundary layer, which inhibits vertical motion. Previous studies have used both global climate and convection-permitting regional models to show that the central to eastern U.S. will experience both increasing CAPE and magnitudes of CIN by the end of the twenty-first century (Rasmussen et al., 2017; Chen et al., 2020; Lepore et al., 2021). These results suggest that increased stability may

reduce weak to moderate storms in the future, but if they can reach their level of free convection, convective storms are likely to be more intense due to larger values of CAPE (Rasmussen et al., 2017). Low-level wind shear is another component that plays a significant role in storm development and organization. Wind shear between the surface and 6km (S06) exerts a profound influence on storm type, organization, and longevity, according to prior studies (Rasmussen and Blanchard, 1998; Weisman and Rotunno, 1999; Brooks et al., 2003).

Changes in convective parameters are useful for exploring potential changes in storm characteristics, and integrated measures, such as the product of CAPE and S06, can provide additional information. This product (CAPES06), by definition, considers both thermodynamic and kinematic variables of relevance to storm environments. An increase in CAPES06, for instance, could indicate an increase in the frequency of significant severe storms (Rasmussen & Blanchard, 1998; Brooks et al., 2003; Brooks, 2009) and organized MCSs.

In this study, we use a large ensemble of Earth system model simulations to explore possible future changes in large-scale convective parameters over SA as a whole, as well as SSA specifically. In the large-ensemble approach, many simulations of the future are run under the same radiative forcing scenario, but with individual ensemble members starting from slightly different initial conditions. This produces a different sequence of unforced (internal or natural) climate variability within each simulation since internal climate variability is largely unpredictable. The result is a set of simulations with a range of possible future outcomes where any possibility can be considered reality (Deser et al., 2012). Internal climate variability provides information on the range of uncertainty in regional climate change projections and can significantly augment or counteract the forced response (Deser, 2020). When examining climate changes several decades into the future, internal climate variability is generally greater in the

extratropics than in the tropics, and it is often stronger than the forced climate change signal (Hawkins & Sutton, 2009; Deser et al., 2012; Milinski et al., 2020).

This study was conducted using a recently released large ensemble of simulations from version 2.0 of the Community Earth System Model (CESM2; Danabasoglu et al., 2020). Utilizing the CESM2-LE (Rodgers et al., 2021), we evaluate the temporal evolution of large-scale convective environments in South America from 1870-2100. The CESM2-LE provides an opportunity to robustly evaluate both the forced variability resulting from anthropogenic climate change and the possible modulation of the forced signal by internal variability.

Chapter 2 Methodology

2.1 Data and Model Simulations

The Community Earth System Model (CESM) is a freely accessible community tool that can be used to study a wide range of Earth system interactions over time and space and has been used by many researchers around the world (Hurrell et al., 2013). CESM is an important model for the climate research community. It is funded primarily by the National Science Foundation (NSF) and managed by National Center for Atmospheric Research (NCAR). The CESM has played a significant role in both national and international assessments of climate science. Version two of the CESM (CESM2; Danabasoglu et al., 2020), for instance, contributed many simulations to Phase 6 of the Coupled Model Intercomparison Project (CMIP6; Eyring et al., 2016). CESM provides researchers with a comprehensive modeling system to explore a multitude of interactions within the Earth system, encompassing many different temporal and spatial scales.

From the CESM2-LE (Rogers et al., 2021), we extracted daily data for column air temperature, specific humidity, near-surface (10-meter) wind speed, zonal and meridional winds, and geopotential height. The CESM2-LE uses the Community Atmosphere Model version 6 (CAM6), configured with 32 vertical levels, a relatively coarse vertical representation of the stratosphere, and a spatial resolution of approximately 1° (1.25° in longitude and 0.9° in latitude; Rodgers et al., 2021). Data covering the time period of 1870-2100 was obtained from the first 50 of 100 ensemble members for the purposes of our study. The ensemble members are based on historical forcing provided by CMIP6, as well as SSP3-7.0 for future forcing (Rodgers et al., 2021). The SSP3-7.0 is considered to be a medium- to high-end of forcing scenario (IPCC, 2021). An ensemble of Earth system model simulations of this magnitude and duration presents an

unparalleled opportunity to examine the long-term evolution of large-scale convective environments. It also allows us to explore the influence of forced variability on these environments and to what extent internal climate variability is likely to modify the forced signals.

While we examine changes in large-scale convective parameters over all of SA, we focus primarily on SSA (Figure 1). We mask ocean regions from all analyses.

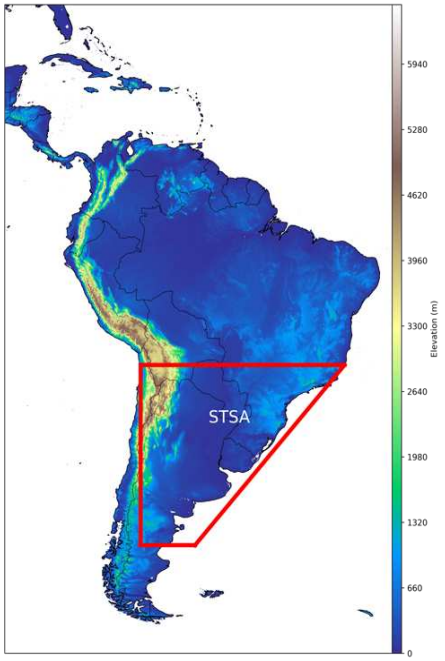

Figure 1: The study focused on the Subtropical South America domain, which encompasses latitudes ranging from -40°S to -20°S and longitudes ranging from -70°W to -45°W.

2.2 Parameters

2.2.1 Convective available potential energy

Convective available potential energy (CAPE) (J/kg) is a thermodynamic parameter that is important for understanding the possible intensity of the convective environment (Riemann-Campe et al., 2009). It is the vertical integral of buoyancy between the level of free convection and the equilibrium level, which is useful for identifying conditional instability and the possibility of strong updrafts (Holton, 1972). To capture potentially elevated convection and the maximum

instability, we compute the most-unstable CAPE in the lowest 3,000 meters (Rochette et al., 1999). Although high levels of CAPE can be present, strong convection may not necessarily occur because the simulated air parcel may need to overcome a stable layer between the surface (SFC) and the level of free convection (LFC; Riemann-Campe et al., 2009).

2.2.2 Convective inhibition

As air parcels ascend from the surface to the lower boundary layer, convective inhibition (CIN) (J/kg) represents the negative buoyancy or negative work done by the atmospheric boundary layer (Colby, 1984; Rasmussen and Blanchard, 1998; Riemann-Campe, 2009). It determines how stable the local atmosphere is and whether convective motion may be suppressed. Due to the fact that CIN represents how much energy an air parcel needs to overcome before reaching the LFC, it is typically defined as a negative value. Therefore, more negative values indicate more stability.

2.2.3 Tropospheric wind shear

Wind shear is one of the important kinematic variables of a convective environment. We computed the parameter S06 (m/s), which is the bulk vertical wind shear from 10 m to 6 km altitude. Previous studies have used this parameter to understand the storm type, severity, and organization (Rasmussen and Blanchard, 1998; Weisman and Rotunno, 1999; Brooks et al., 2003). Larger values of S06 are typically associated with thunderstorms with strong mid-level rotation. Such storms display enhanced storm dynamics, such as an upward-tilted updraft that displaces the upward vertical motion from the downward vertical motion. For an isolated supercell, high S06 increases the likelihood of severe impacts, such as tornadoes. To counteract the low-level circulation induced by the cold pool, sufficient S06 is critical for the formation of multi-cellular organized systems, such as squall lines (Rotunno et al., 1988). The development of new cells is

triggered by the gust front, and their subsequent growth is highly dependent on the amount of low-level wind shear, which plays a crucial role in the longevity of multi-cellular organized systems.

2.2.4 CAPES06

The thermodynamic and kinematic parameters mentioned above are important, but it is also useful to examine the product of CAPE and S06 (CAPES06). This parameter is useful to differentiate between ordinary and severe storms, and it has been used by many researchers and forecasters previously to evaluate severe local storm environments (Rasmussen and Blanchard, 1998; Craven and Brooks, 2002; Brooks et al., 2003; Brooks, 2009; Seeley and Romps, 2015). Higher magnitudes of CAPES06 suggest augmented potentials for storm organization and greater updraft velocities, which can potentially lead to a severe thunderstorm. Previous studies that examined soundings from severe thunderstorm environments showed that such storms were typically associated with higher values of CAPES06 (Rasmussen and Blanchard, 1998; Brooks et al., 2003; Brooks, 2009, Schumacher et al., 2021).

2.3 Model Verification

We use the fifth-generation global climate reanalysis (ERA5) (Hersbach et al., 2020) from the European Centre for Medium-Range Forecast (ECMWF) to examine the fidelity of CESM2 in the context of large-scale convective weather parameters. ERA5 has been shown to reliably capture the global spatiotemporal climatology of convective environments (Taszarek et al., 2021). In addition, Franke et al. (2022) showed that CESM2-LE is a reliable model to examine changes in large-scale convective environments over North America. Moreover, prior research has undertaken a climatological analysis of severe local storm environments across North America, employing a comparison between ERA5 and CAM6 simulations from the historical period (Li et

al., 2020). They verified the accuracy of ERA5 by comparing it against 69 radiosonde observations over the CONUS region, which included twice daily raw soundings.

To compare the model data with reanalysis data, we first compute the climatology of CAPE for both datasets. Figure 2 shows the CAPE climatology in the austral spring and summer (SONDJF) from 1980-2019 for the CESM2-LE and ERA5. Note that the model climatology is computed from 50 ensemble members, or 2,000 simulated years in total, whereas ERA5 is based on only 40 years of data. Nonetheless, the spatial distribution from CESM2 is similar to that from ERA5, with the highest values over the Amazon region. Forested areas are less stable and have higher values of CAPE, which is attributed to the increased humidity levels in these areas (Wang et al., 2009). Although not shown, a similarly strong agreement was found between ERA5 and CESM2-LE for the climatological distributions of CIN, S06, and CAPES06.

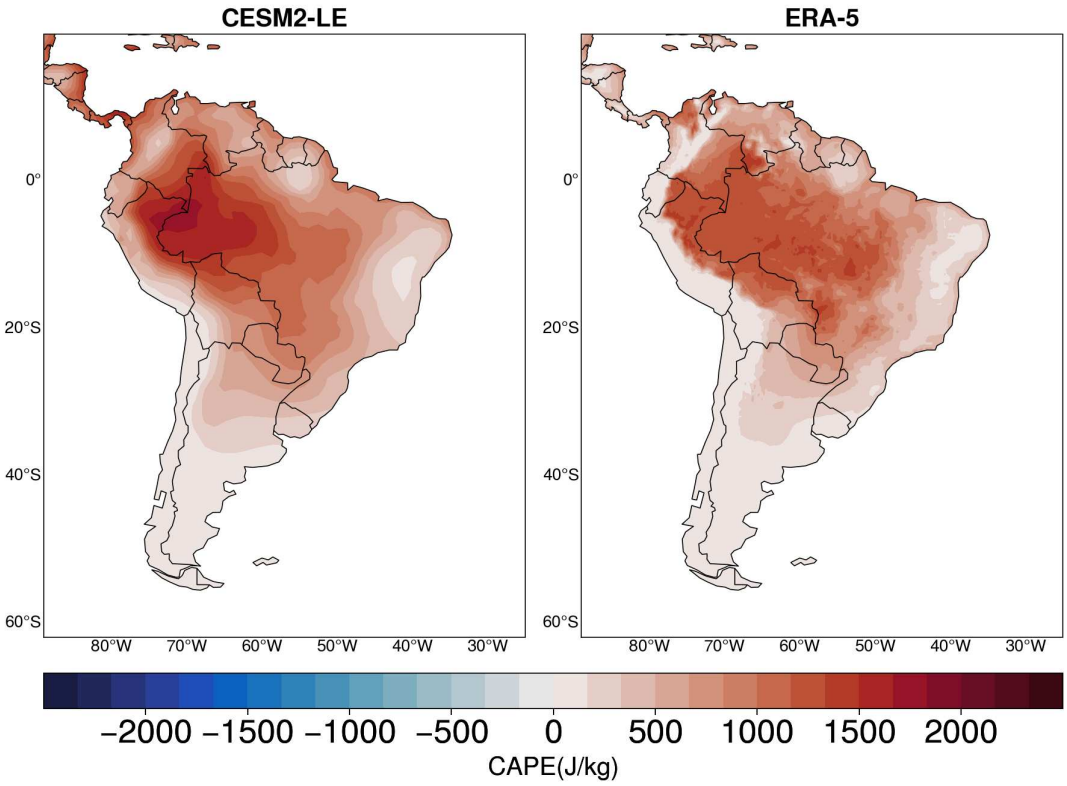

Figure 2: Climatology of SONDJF CAPE for CESM2-LE (left) and ERA5(right) from 1980-2019.

In addition to climatological distributions of large-scale convective parameters, it is useful to examine how well CESM2 captures modes of climate variability. Large-scale modes of natural climate variability influence weather and climate from sub-seasonal to interdecadal time scales. The El Niño-Southern Oscillation (ENSO) phenomenon, for instance, has been found to have a significant connection to the occurrence of severe weather events (Cook et al., 2017; Cook & Schaefer, 2008; Tippett et al., 2015; Bruick et al., 2019). The relationship between CAPE and ENSO from ERA5 and CESM2 is shown in Figure 3. In particular, we examine the regression of austral spring and summer (SONDJF) CAPE from CESM2-LE onto the simulated Nino 3.4 index and ERA5 onto the observed Nino 3.4 index. The model data covers the period of 1870-2019 to increase the sample size, relative to only 1980-2019 from ERA5; however, the results are very similar if only the simulated 1980-2019 period is examined from the CESM2-LE (not shown).

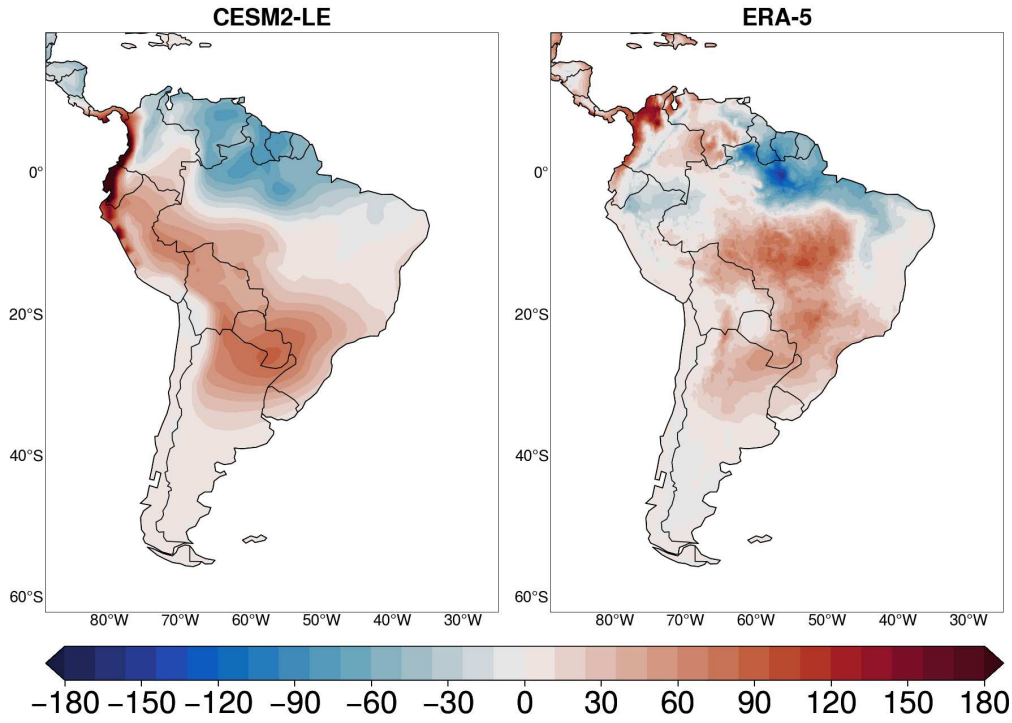

Figure 3: One standard deviation regression of CAPE onto the ENSO index over the SONDJF from CESM2-LE (1870-2019; left) ERA5 reanalysis (1980-2019; right).

Importantly, the CESM2-LE effectively captures the primary shifts in CAPE attributed to ENSO. These include a significant enhancement of CAPE over SSA during warm ENSO phases alongside lower values of CAPE over the northeast region of SA. While not explored in detail here, we further note that CESM2 well simulates modes of variability that operate on longer-time scales as well (e.g., Danabasoglu et al., 2020; Simpson et al., 2020). For instance, the model exhibits a spatial pattern of the Pacific Decadal Oscillation (PDO) that closely aligns with observed patterns (Capotondi et al., 2020; Wei et al., 2018).

We also evaluated the relationship between global sea surface temperature (SST) variability and variations in large-scale convective parameters area-averaged over the SSA region during SONDJF to see how effectively the model can capture the changes in convective parameters associated with SST. Over the historical period (1870-2019), there is a strong relationship between the convective parameters and eastern Pacific SST (Figure 4), which illustrates the importance of this oceanic region to interannual and longer-term climate variations in the SSA region. Previous studies have also indicated a strong relationship between deep convection and severe weather over SSA with different phases of the ENSO (e.g., Bruick et al., 2019). During El Niño, for instance, convective storms are typically characterized by greater heights and more intense precipitation compared to the storms during La Nina. On the other hand, during La Nina events, deep and wide convective cores (DWCC) exhibit enhanced stratiform reflectivity below the melting level, which results in intensified rainfall (Bruick et al., 2019).

Finally, the regression of CAPE area-averaged over SSA onto global SST from ERA5 (1980-2019) is shown in Figure 5B, for comparison with Figure 4A. It is evident that CESM2 captures overall regression patterns evident in the reanalysis. The findings presented in this section, as well as those from previous studies, provide us with confidence in utilizing the CESM2-LE to

investigate both historical and future forced and internal changes in large-scale convective environments over SA, including the SSA region specifically (Figure 1).

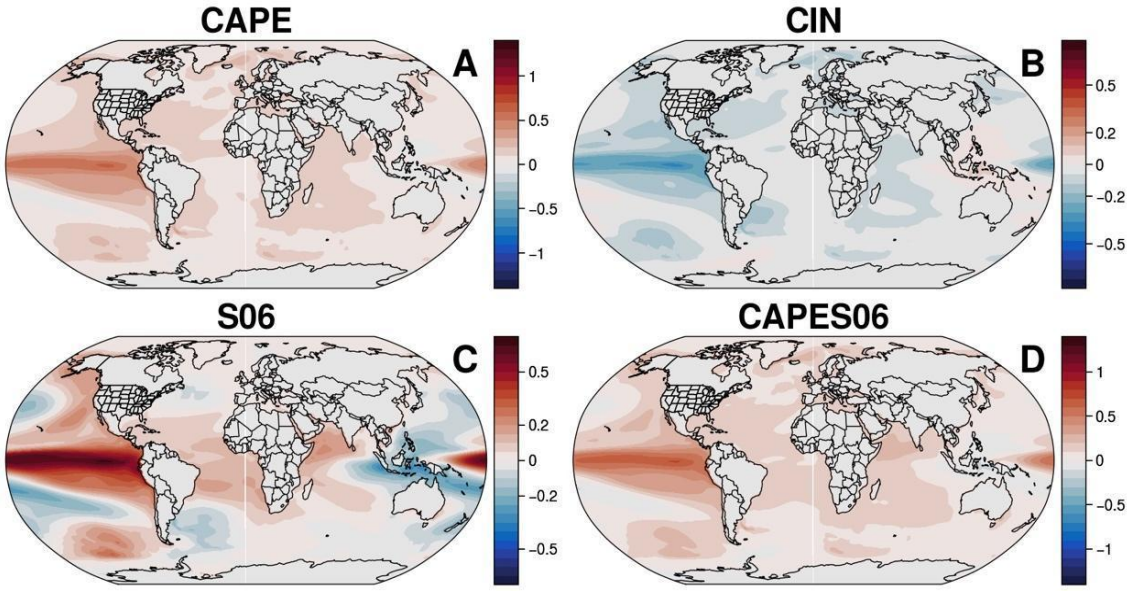

Figure 4: Regression of (A) CAPE, (B) CIN, (C)S06, (D)CAPES06 from 1870-2019 over subtropical South America during spring and summer (Sep-Feb) onto global SST.

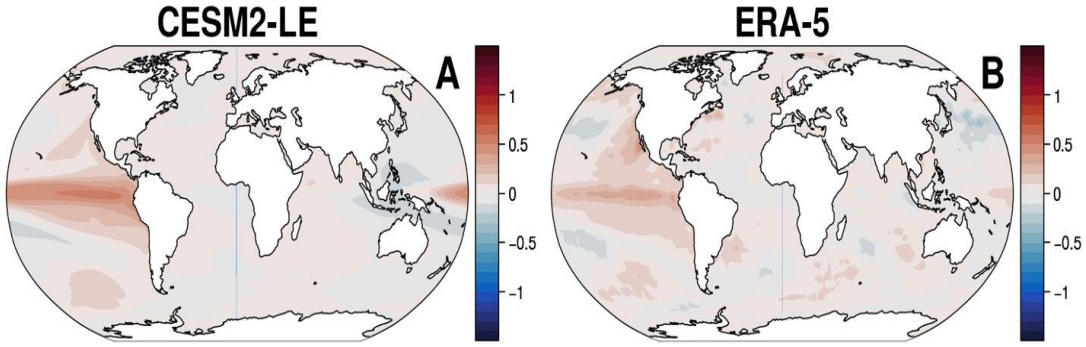

Figure 5: Regression of SSA CAPE onto global SST for CESM2-LE (A) from 1870-2019 and ERA5(B) from 1980-2019.

Chapter 3 Results and Discussions

3.1 Ensemble Mean (Forced Change) Results Over South America

We begin by evaluating the annual historical and future changes in large-scale convective parameters from 1870-2100 averaged over the South American continent. In the time series, anomalies are expressed relative to the 30-year base period of 1971-2000 (Figure 6). Variations of the forced component of climate change are given by the 50-member ensemble mean time series (dark lines). Considerable interannual and decadal variability is evident in the time series of individual ensemble members. Forced changes in CAPE, CIN, and CAPES06 are not apparent in any of the parameters until late in the 20th century when increases in the magnitude of CAPE, CIN, and CAPES06 begin and continue through the 21st century. Averaged over all of SA, S06 exhibits no significant trend because, as shown later (Figure 9), there are regions of both positive and negative S06 trends across the continent. It is also apparent from Figure 6 that anthropogenic forcing produces changes in convective environments in nearly all of the 50 individual members of CESM2-LE. Therefore, it is very likely that the convective environment over SA as a whole will have higher convective energy, but with more stability which is consistent with previous studies in the U.S. (Rasmussen et al., 2017).

The spatial patterns of seasonal trends across the continent over the next 30 years (2020-2049) are presented in Figures 7-10. During the austral summer (DJF), the whole continent exhibits an increase in CAPE except for the far north (Figure 7A). Likewise, during fall (MAM) most of the continent shows a positive trend, with the largest increase in CAPE over northwest Brazil and southern Colombia (Figure 7B). During winter (JJA) there is little change projected over the next

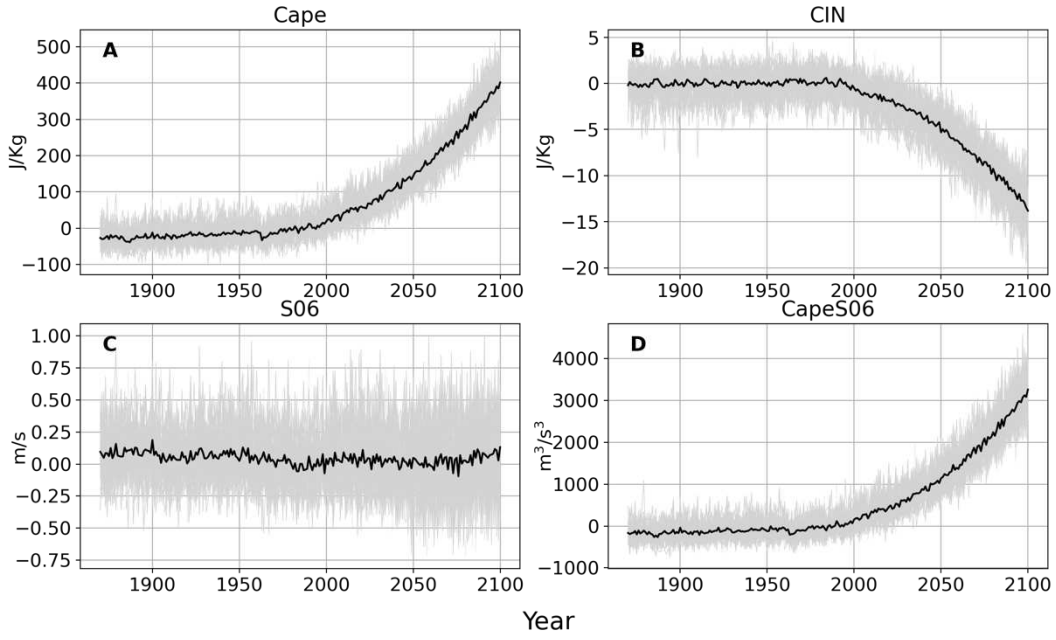

Figure 6: Time series of anomalies of the annual mean (A) CAPE, (B) CIN, (C) S06, (D) CAPES06 from 1870-2100 relative to the 30-year base period of 1971-2000 averaged over South America. The 50-member ensemble mean is shown in the thick black lines and the individual members are shown in light gray lines.

30 years in CAPE over most of the continent, except in the tropical region that remains warm throughout the year (Figure 7C). During spring (SON), positive trends are evident in South Colombia and Venezuela, as well as in the subtropical region of the continent in Paraguay, Argentina, and southern Brazil (Figure 7D). Previous studies have projected similar seasonal patterns of change in CAPE in SA (Lepore et al., 2021). Projections indicating higher CAPE suggest the potential for more intense and explosive convection in the near-term future.

Seasonal trends in CIN over the coming decades are shown in Figure 8. During the austral summer and fall, the projected forced changes are characterized by a decrease over much of SA, especially over the SSA region and northwest Brazil (Figure 8A, B). No noticeable trends are

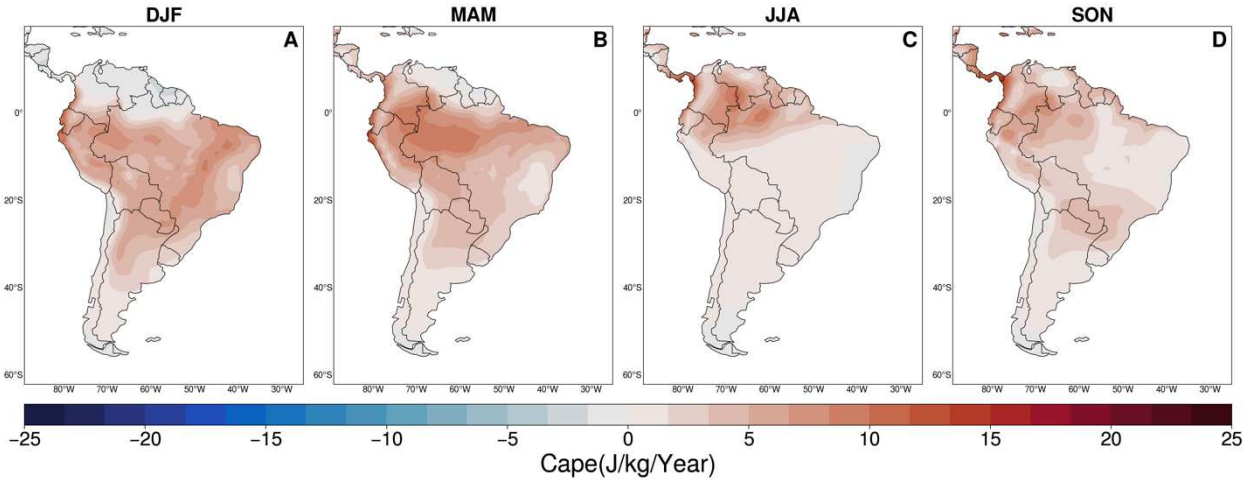

Figure 7: Seasonal linear trends for CAPE from 2020-2049 over South America for 50-ensemble mean. (A) DJF, (B) MAM, (C) JJA, (D) SON.

evident during winter (Figure 8C), but by spring declines in CIN are again evident, especially over subtropical South America (Figure 8D). Once again, these changes are broadly consistent with those shown recently by (Lepore et al., 2021), as well as from both high-resolution regional and global climate modeling studies in the U.S. (Rasmussen et al., 2017; Chen et al., 2020). A decrease in CIN indicates a more stable or capped atmosphere. Strong CIN is capable of inhibiting convection completely and moderate CIN can lead to an accumulation of CAPE, which can result in explosive convection if rising parcels can eventually reach their LFC.

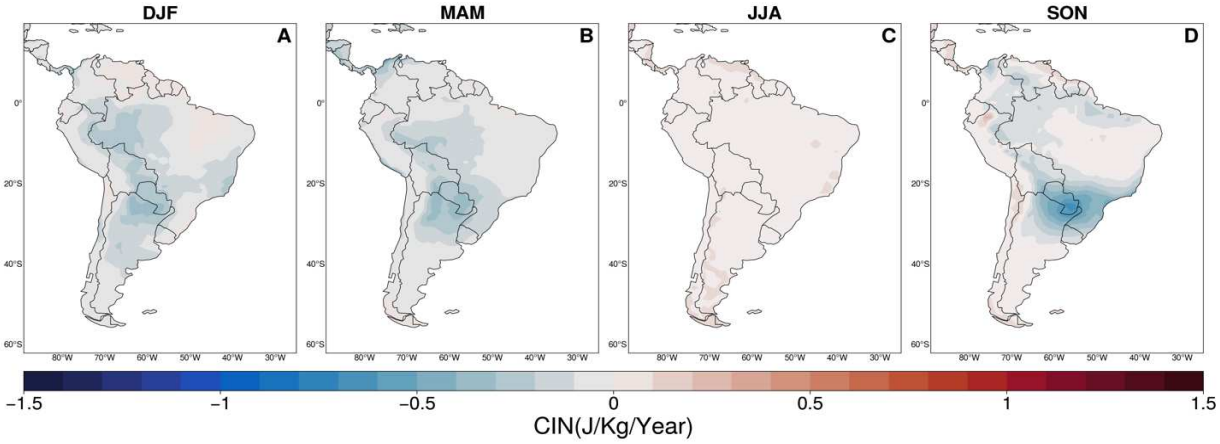

Figure 8: Seasonal linear trends for CIN from 2020-2049 over South America for 50-ensemble mean. (A) DJF, (B) MAM, (C) JJA, (D) SON.

The forced component of the trend in S06 during the summer shows a positive trend over most of the continent except for southern SA (Figure 9A). Over the next 30 years, the increase in lower tropospheric wind shear is the largest in the subtropical regions for all seasons. During fall and winter, S06 across tropical latitudes decreases (Figure 9B, 9C). During spring, southeast Brazil exhibits a decreasing trend in wind shear (Figure 9D). These regions of positive and negative trends across the continent explain why no significant change was seen in the time series of S06 averaged over all of SA (Figure 6C).

Environments characterized by large vertical shear favor storms with vertical rotation and deeper, more intense updrafts. Such ingredients are important for the genesis of tornadic storms, along with large hail and damaging outflow winds at the surface (Weisman and Rotunno, 2000; Trapp et al., 2007). In addition, such environments favor longer-lasting, self-sustaining, and more organized storms (e.g., Lilly, 1979; Rotunno, 1981; Klemp, 1987; Weisman and Rotunno, 2000). An important question to examine is the origin of the banded structure in S06 evident in Figure 9. A possible explanation is provided by examining concurrent changes in tropical rainfall, which exhibit projected increases in the equatorial eastern Pacific rainfall throughout all seasons over the next 30 years. Such enhanced convective heating enhances upper-level divergence over the equatorial eastern Pacific, and the anomalous vorticity drives the propagation of Rossby wave trains into the extratropics (Sardeshmukh and Hoskins, 1988; Qin and Robinson, 1993). Indeed, spatial patterns of 300 hPa zonal wind trends across SA exhibit alternating bands of increasing and decreasing winds originating from the tropical eastern Pacific, aligning with this concept. This provides support for the notion that future variations in S06 are primarily driven by future changes in tropical precipitation in the CESM2, although questions exist as to whether or not such rainfall changes are realistic (e.g., Seager et al., 2022; Yin et al., 2013; Fiedler et al., 2020).

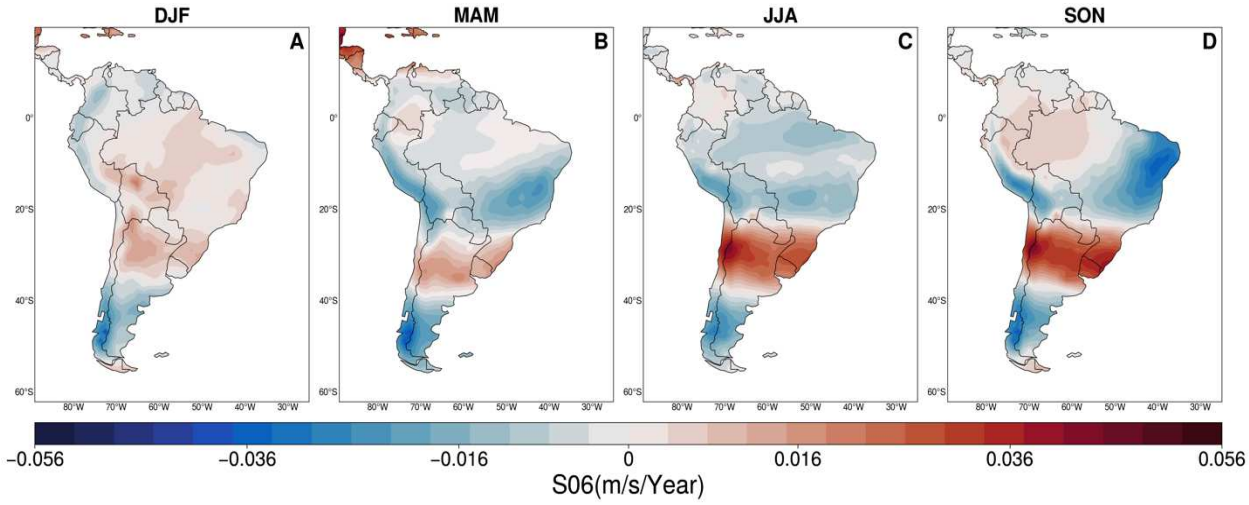

Figure 9: Seasonal linear trends for S06 from 2020-2049 over South America for 50-ensemble mean. (A) DJF, (B) MAM, (C) JJA, (D) SON.

Regardless, spatial patterns of trends in CAPES06 over SA are dominated by changes in CAPE, as is evident by comparing Figures 7 and 10. In regions where CAPES06 shows an increasing trend, there is a greater probability of significant severe storms, especially over SSA during summer, fall, and spring.

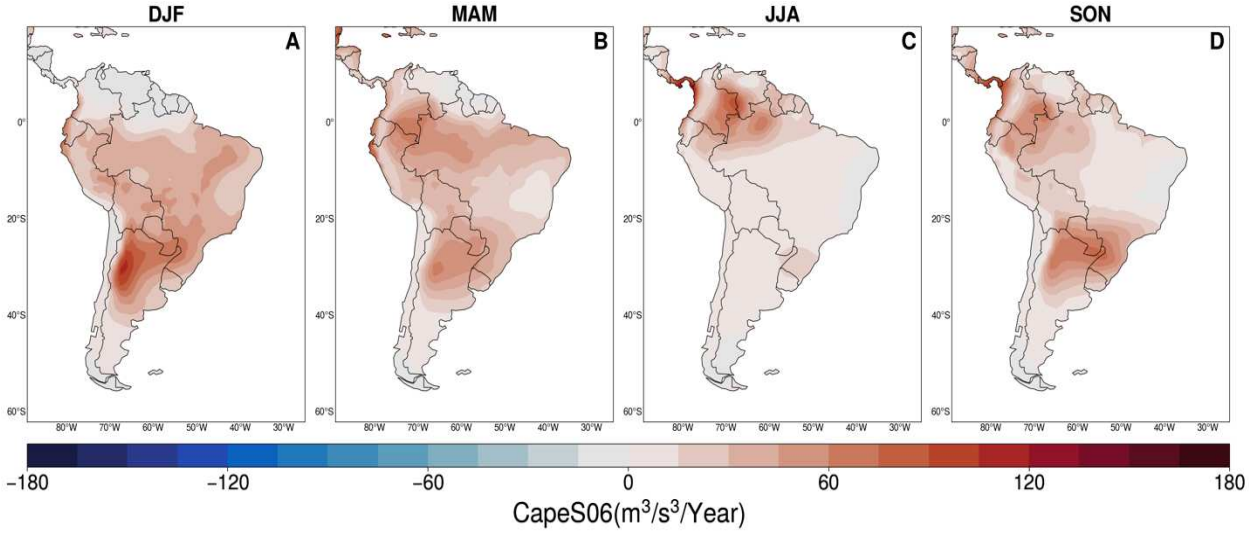

Figure 10: Seasonal linear trends for CAPES06 from 2020-2049 over South America for 50-ensemble mean. (A) DJF, (B) MAM, (C) JJA, (D) SON.

3.2 Forced changes over subtropical South America

Given the frequent occurrence of intense convection across SSA, particularly during the six months of austral spring and summer (September to February), we next focus on this region in more detail. In particular, the time series analysis presented in Figure 6 averaged across all of SA is repeated in Figure 11 for just SSA. The forced component of CAPE over this region is projected to exhibit a steady increase, leading to a rise of ~ 550 J/kg by 2100 (Figure 11A). CIN is projected to increase in magnitude and reach ~ -15 J/kg by the end of the century (Figure 11B). Additionally, the forced positive change in S06 through 2049 in Figure 9 continues through the end of the century, reaching ~0.85m/s by 2100 relative to the reference period (Figure 11C). CAPES06 shows a similar trend as CAPE with a linear increase of ~7400m^3/s^3 by 2100 (Figure 11D).

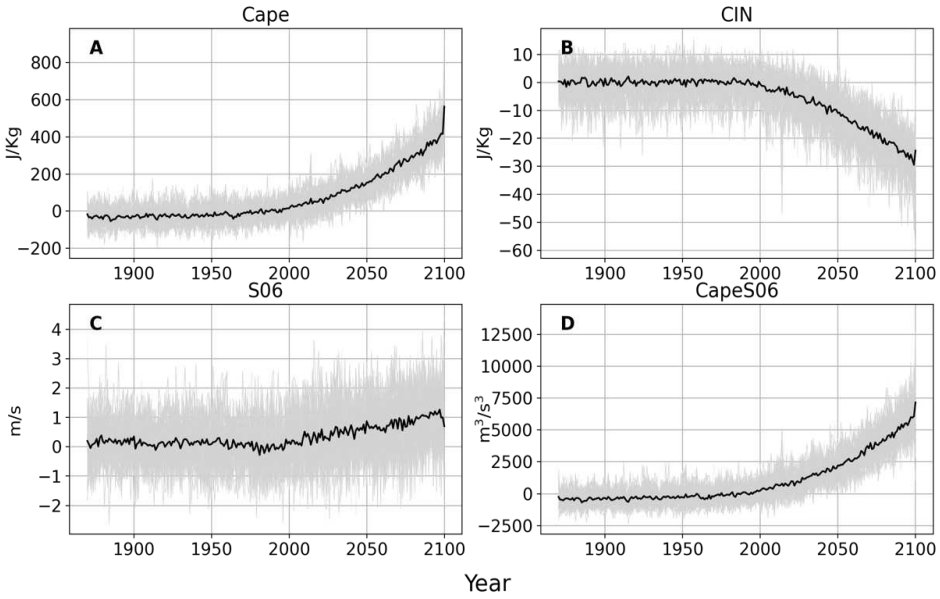

Figure 11: Time series of austral spring and summer (September to February) anomalies of (A) CAPE, (B) CIN, (C) S06, (D) CAPES06 from 1870-2100 relative to the 30-year base period of 1971-2000 averaged over subtropical South America (SSA). The 50-member ensemble mean is shown in black lines and the individual members are shown in light gray lines.

Over the SSA region, there is a vertical motion pattern broadly characterized by upward motion on the windward side of the Andes and downward motion on the leeward side (Rasmussen et al., 2011). This vertical motion pattern is primarily influenced by the mean westerlies crossing the mountains at these latitudes. This downward motion effectively inhibits convection east of Andes (Rasmussen et al., 2011), and it explains the high CIN in the subtropical latitudes. A higher amount of CAPE is needed to break this capping inversion, which would indicate an environment that would favor the development of severe weather. Rasmussen et al., (2016) showed that in terrain modification experiments with the Andes decreased by 50%, reduced magnitudes of both CIN and CAPE resulted. Thus, the extreme height of the Andes leads to important thermodynamic environments supporting convective storms in the region that differ from environments in the U.S., despite similarities in flow features and MCSs across both regions (Velasco and Fritsch, 1987; Rasmussen et al., 2011).

3.3 Internal Climate Variability

The utilization of the CESM2-LE presents a unique opportunity to fully explore the influence of internal or unforced climate variability and how it might modify the forced responses described above with each of the 50 ensemble members representing an equally plausible trajectory. This approach allows us to illustrate the range of possible regional climate outcomes that is not possible with high-resolution regional climate model simulations (Liu et al., 2016) due to limitations in computational time. We analyze the linear trends in each of the convective indices over the next 30 years (2020-2049) averaged over SSA. Histograms of these trends across the 50-member ensemble are a simple metric that depicts the extent to which internal climate variability

drives climate outcomes that differ from considering the anthropogenic climate change signal only (Figure 12).

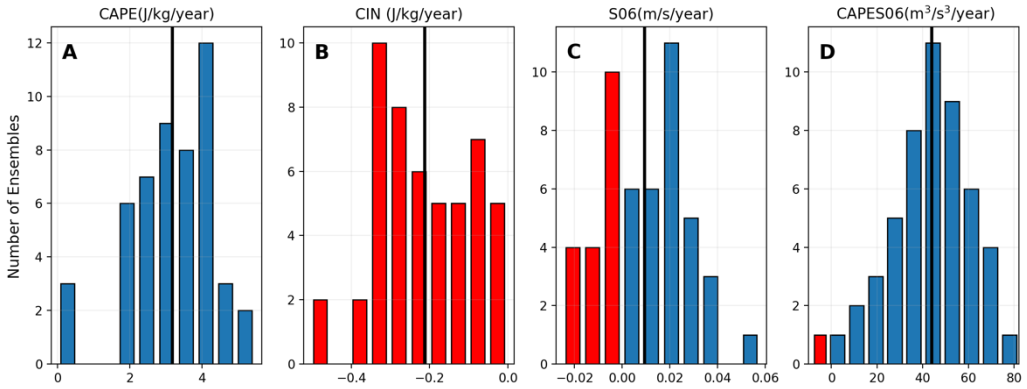

Figure 12: Histogram showing the spread of linear trends per year for the period of 2020-2049 during the month of September-February across the 50-member CESM2-LE for (A) CAPE, (B) CIN, (C) S06, (D) CAPES06. Red colored bars indicate negative values. The black line indicates the ensemble mean value.

The substantial influence of internal variability is clear in each convective parameter histogram. For CAPE averaged over SSA, for instance, trends range from 0 to ~5 J/Kg/year, and two-thirds of the ensemble members have trends between 2 and 4 J/Kg/year (Figure 12A). Despite this large range, all 50 ensemble members exhibit a positive trend in CAPE. Similarly, the 30-year trend in CIN is negative for all ensemble members (Figure 12B), but trends for individual members range from near 0 to ~ -0.5 J/Kg/year. In contrast, the 30-yr linear trends in S06 show both positive and negative values (Figure 12C), with 32 ensemble members displaying positive trends and 18 exhibiting negative trends. Trends in CAPES06 from individual ensemble members are dominated by CAPE, and thus the majority (except one) are positive. Additionally, 84% (42 out of 50) of the ensemble members exhibit trends ranging from 20 to 60 J/kg/year (Figure 12D). The histograms presented here demonstrate the range of uncertainty associated with trends in convective

parameters over the SSA region in the coming decades, despite there being clear trends in these parameters due to greenhouse gas forcing (Figure 11).

To further illustrate the importance of considering internal climate variability in future climate projections, we subjectively select the ensemble members with the largest and smallest trends in area-averaged austral spring and summer (SONDJF) CAPE over SSA to examine the spatial patterns of change in those ensemble members (Figure 13). Recall that all ensemble members in the CESM2-LE experience identical changes over time with respect to greenhouse gas forcing; consequently, differences in the spatial patterns of individual simulations can be attributed to different evolutions of their internal climate variability. By simply subtracting the forced component from the ensemble mean, the contributions to changes in CAPE due to internal climate variability alone is revealed (Figures 13B, E) from each ensemble member (Figures 13C, F). It is notable that changes in CAPE due to internal climate variability alone exhibit spatially coherent structures over large regions that are of the same general magnitude as the forced trends. This is true for all 50 ensemble members (not shown), even though we illustrate it here for the ensemble members with the largest and smallest trends in CAPE averaged over SSA.

As for CAPE, we examine the spatial trends in CIN for the same two ensemble members (#19 and #39; Figure 14). Over the next several decades, CIN increases in magnitude across southern Brazil, northern Argentina, and Paraguay in ensemble member 19. If this is how the real world unfolds, which is entirely plausible, the capping inversion would strengthen and thus convection would be inhibited. Moreover, internal climate variability drives an increasing trend in CAPE (Figure 13A), so that there is more energy available for convective activity. Despite this, many air parcels may not possess the required strength to breach the capping inversion, which would lead to a reduction in the occurrence of weak to moderate storms and an increase in strong

to extreme storms. In this scenario, the internal climate variability amplified the forced changes over SSA. In contrast, for ensemble member 39, trends induced by internal climate variability counteract the forced changes (Figure 14D).

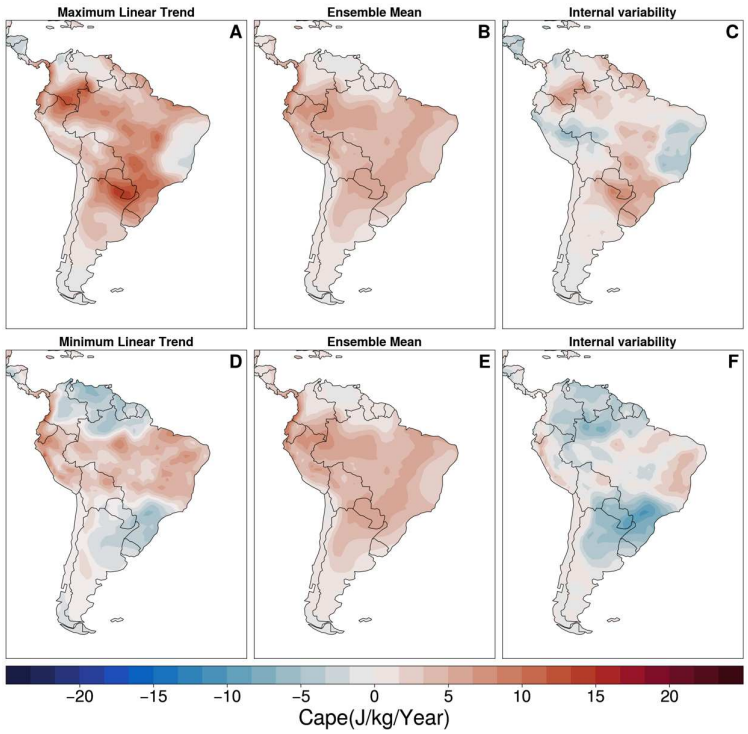

Figure 13: Linear trends in CAPE (2020-2049) over SA during Sep-Feb for ensemble numbers 19 (top) and 39 (bottom). The middle column shows the forced trend and the right column shows the trend due solely to internal variability.

Finally, the spatial trends of S06 for the same two ensemble members are shown in Figure 15. Ensemble member 19 exhibits a weakening of low-level wind shear in central Argentina (Figure 15A), which might contribute to less organized storms, while ensemble member 39 (Figure 15D) shows an increasing trend, suggesting enhanced storm organization. For ensemble member 19, internal variability counteracts the forced change, resulting in negative changes in the subtropical region. In the case of ensemble member 39, the impact of internal variability is more intricate. In the region encompassing northern Argentina and southern Brazil, internal variability opposes the forced change, leading to negative changes. However, in central Argentina, internal

variability amplifies the forced change, resulting in an increase in that region. Based on the findings presented, it is evident that forced response may make the convective environment in SSA more supportive of less frequent but longer-lasting and more organized convective storms and the forced response is likely to be considerably moderated by internal climate variability.

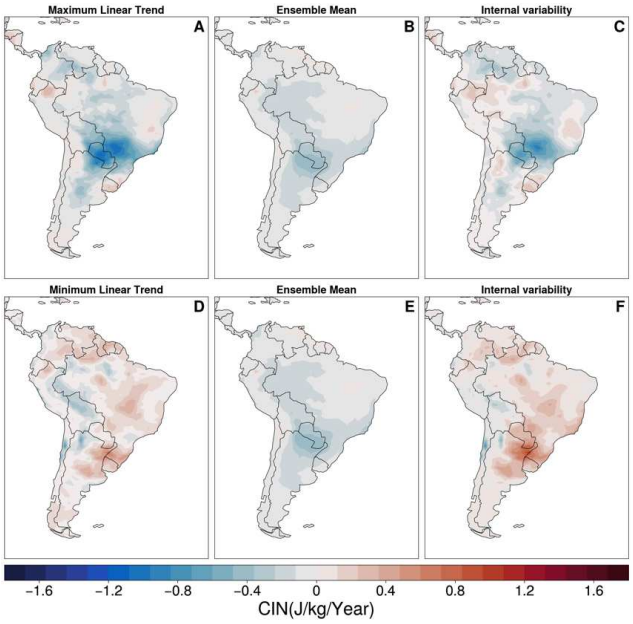

Figure 14: Same as Figure 13, except for CIN.

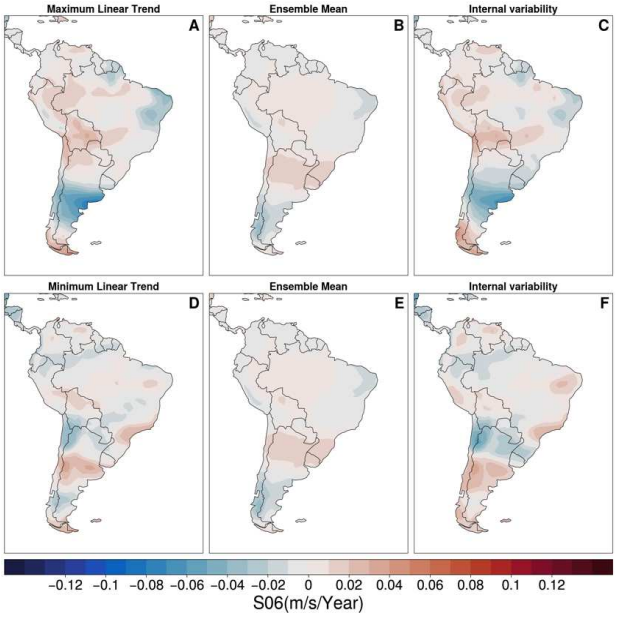

Figure 15: Same as Figure 13, except for S06.

Chapter 4 Conclusions

A 50-member ensemble of Earth system climate model simulations is used to understand the potential changes in thermodynamic and kinematic environments supporting severe and hazardous weather in a warmer, future climate over SA. By utilizing the CESM2-LE, we not only identified and analyzed anthropogenically-induced changes in large-scale convective environments over time, but we have also documented how internal (unforced) climate variability is likely to modify the forced changes. To our best knowledge, this particular aspect has not been thoroughly documented before for SA. Better understanding the potential range of future changes in convective environments can improve our ability to forecast and prepare for severe weather events. Specifically, such knowledge can enhance resilience and preparedness to face such hazards.

In our study, we used an exceptionally well-documented Earth system model - the second version of the Community Earth System Model (CESM2) - to analyze the temporal evolution and spatial trends of different convective parameters over SA from 1870-2100. Our results show that anthropogenic climate change is expected to shift the future convective environments in such a way as to favor a decrease in frequency, but an increase in intensity, of convection, especially over SSA. Moreover, over this region, there could be more kinematic support that could potentially lead to more favorable conditions for the formation of convective storm modes capable of generating very severe weather events.

We also examined the influence of internal climate variability on large-scale convective environments. Results clearly illustrated that internal variability will be significant, and it needs to be considered in future projections of climate change over SA. In particular, unforced climate

variability on decadal time scales drives large, spatially coherent changes over large regions of SA that can significantly modify the climate response to anthropogenic forcing. Nevertheless, it is important to point out that the validity of our results rests on the capability of the CESM2 to realistically simulate future conditions. This has been demonstrated in previous studies, for instance, that examine the fidelity in which CESM2 simulates modes of natural climate variability from sub-seasonal through multi-decadal time scales. Here, we also examined how well CESM2 replicates the observed climatological distribution of large-scale convective parameters, as well as its ability to simulate spatial changes associated with ENSO (e.g., Figure. 2, 3,4,5). Additionally, we point out that our results are for a single future forcing scenario (SSP3-7.0).

In future work, we intend to conduct a more thorough regional analysis as different regions are influenced differently by both forced and internal climate variability. Moreover, further investigation is needed to understand the large-scale circulation changes that drive internal variations in convective indices and their potential connection to coupled modes of climate variability. It would also be important to determine the predictability associated with internal variability in such cases. Additionally, similar analysis can be done for different regions of the globe, for example, the northwestern Himalayas (Rasmussen et al., 2011). Franke et al. (2022) have also used the CESM2-LE to examine future changes in convective parameters of the eastern United States during boreal spring and summer. Gaining a comprehensive understanding of the potential future evolution and variability in large-scale convective environments is of utmost importance in order to document possible forthcoming changes in severe weather hazards. Such knowledge is crucial for making informed decisions on how to effectively adapt to and mitigate the impacts of these high-impact hazards.

References

Brooks, H. E. (2009). Proximity soundings for severe convection for Europe and the United States from reanalysis data. *Atmospheric Research*, *93*(1–3), 546–553. https://doi.org/10.1016/j.atmosres.2008.10.005

Brooks, H. E., Lee, J. W., & Craven, J. P. (2003). The spatial distribution of severe thunderstorm and tornado environments from global reanalysis data. *Atmospheric Research*, *67–68*, 73–94. https://doi.org/10.1016/S0169-8095(03)00045-0

Bruick, Z. S., Rasmussen, K. L., Rowe, A. K., & McMurdie, L. A. (2019). Characteristics of intense convection in subtropical South America as influenced by El Niño-Southern oscillation. *Monthly Weather Review*, *147*(6), 1947–1966. https://doi.org/10.1175/MWR-D-18-0342.1

Cai, W., McPhaden, M. J., Grimm, A. M., Rodrigues, R. R., Taschetto, A. S., Garreaud, R. D., Dewitte, B., Poveda, G., Ham, Y.-G., Santoso, A., Ng, B., Anderson, W., Wang, G., Geng, T., Jo, H.-S., Marengo, J. A., Alves, L. M., Osman, M., Li, S., Wu, L., Karamperidou, C., Takahashi, K., & Vera, C. (2020). Climate impacts of the El Niño–Southern Oscillation on South America. Nature Reviews Earth & Environment, 1(6), 315-328. https://doi.org/10.1038/s43017-020-0040-3

Campetella, C. M., & Vera, C. S. (2002). The influence of the Andes mountains on the South American low-level flow. *Geophysical Research Letters*, *29*(17), 6–9. https://doi.org/10.1029/2002GL015451

Capotondi, A., Deser, C., Phillips, A. S., Okumura, Y., & Larson, S. M. (2020). ENSO and Pacific Decadal Variability in the Community Earth System Model Version 2. *Journal of*

Advances in Modeling Earth Systems, *12*(12). https://doi.org/10.1029/2019MS002022

Carlson, T. N., Benjamin, S. G., Forbes, G. S., & Li, Y. (1983). Elevated Mixed Layers in the Regional Severe Storm Environment: Conceptual Model and Case Studies, *Monthly Weather Review*, *111*(7), 1453-1474. https://doi.org/10.1175/1520-0493(1983)111<1453:EMLITR>2.0.CO;2

Chen, J., Dai, A., Zhang, Y., & Rasmussen, K. L. (2020). Changes in convective available potential energy and convective inhibition under global warming. *Journal of Climate*, *33*(6), 2025–2050. https://doi.org/10.1175/JCLI-D-19-0461.1

Colby , F. P., Jr. (1984). Convective Inhibition as a Predictor of Convection during AVE-SESAME II, *Monthly Weather Review*, *112*(11), 2239-2252.https://doi.org/10.1175/1520-0493(1984)112<2239:CIAAPO>2.0.CO;2

Cook, A. R., Leslie, L. M., Parsons, D. B., & Schaefer, J. T. (2017). The impact of El Niño Southern Oscillation (ENSO) on winter and early spring U.S. tornado outbreaks. *Journal of Applied Meteorology and Climatology*, *56*(9), 2455–2478. https://doi.org/10.1175/JAMC-D-16-0249.1

Cook, A. R., & Schaefer, J. T. (2008). The relation of El Niño-Southern Oscillation (ENSO) to winter tornado outbreaks. *Monthly Weather Review*, *136*(8), 3121–3137. https://doi.org/10.1175/2007MWR2171.1

Craven, J. P., & Brooks, H. E. (2004). Baseline climatology of sounding derived parameters associated with deep, moist convection. *National Weather Digest*, *28*, 13–24.

Danabasoglu, G., Lamarque, J.-F., Bacmeister, J., Bailey, D. A., DuVivier, A. K., Edwards, J., Emmons, L. K., Fasullo, J., Garcia, R., Gettelman, A., Hannay, C., Holland, M. M., Large, W. G., Lauritzen, P. H., Lawrence, D. M., Lenaerts, J. T. M., Lindsay, K.,

Lipscomb, W. H., Mills, M. J., Neale, R., Oleson, K. W., Otto-Bliesner, B., Phillips, A. S., Sacks, W., Tilmes, S., van Kampenhout, L., Vertenstein, M., Bertini, A., Dennis, J., Deser, C., Fischer, C., Fox-Kemper, B., Kay, J. E., Kinnison, D., Kushner, P. J., Larson, V. E., Long, M. C., Mickelson, S., Moore, J. K., Nienhouse, E., Polvani, L., Rasch, P. J., & Strand, W. G. (2020). The Community Earth System Model Version 2 (CESM2). *Journal of Advances in Modeling Earth Systems*, *12*(2), 1–35. https://doi.org/10.1029/2019MS001916

Deser, C. (2020). Certain uncertainty: The role of internal climate variability in projections of regional climate change and risk management. *Earth's Future*, *8*(12), e2020EF001854. https://doi.org/10.1029/2020EF001854

Deser, C., Knutti, R., Solomon, S., & Phillips, A. S. (2012). Communication of the role of natural variability in future North American climate. *Nature Climate Change*, *2*(11), 775–779. https://doi.org/10.1038/nclimate1562

Deser, C., Phillips, A., Bourdette, V., & Teng, H. (2012). Uncertainty in climate change projections: The role of internal variability. *Climate Dynamics*, *38*(3-4), 527–546. https://doi.org/10.1007/s00382-010-0977-x

Durkee, J. D., Mote, T. L., & Shepherd, J. M. (2009). The contribution of mesoscale convective complexes to rainfall across subtropical South America. *Journal of Climate*, *22*(17), 4590–4605. https://doi.org/10.1175/2009JCLI2858.1

Eyring, V., Bony, S., Meehl, G. A., Senior, C. A., Stevens, B., Stouffer, R. J., & Taylor, K. E. (2016). Overview of the Coupled Model Intercomparison Project Phase 6 (CMIP6) experimental design and organization. *Geoscientific Model Development*, *9*(5), 1937–1958. https://doi.org/10.5194/gmd-9-1937-2016

Fiedler, S., Crueger, T., D'Agostino, R., Peters, K., Becker, T., Leutwyler, D., Paccini, L., Burdanowitz, J., Buehler, S. A., Cortes, A. U., Dauhut, T., Dommenget, D., Fraedrich, K., Jungandreas, L., Maher, N., Naumann, A. K., Rugenstein, M., Sakradzija, M., Schmidt, H., Sielmann, F., Stephan, C., Timmreck, C., Zhu, X., & Stevens, B. (2020). Simulated Tropical Precipitation Assessed across Three Major Phases of the Coupled Model Intercomparison Project (CMIP), Monthly Weather Review, 148(9), 3653-3680. https://doi.org/10.1175/MWR-D-19-0404.1

Franke, M. E. (2022). Impact of forced and internal climate variability on changes in convective environments over the eastern united states (Order No. 29259848). Available from Dissertations & Theses @ Colorado State University; ProQuest Dissertations & Theses Global. (2705485619). Retrieved from https://ezproxy2.library.colostate.edu/login?url=https://www.proquest.com/dissertations-theses/impact-forced-internal-climate-variability-on/docview/2705485619/se-2

Garreaud, R. D. (2009). The Andes climate and weather. *Advances in Geosciences*, *22*, 3–11. https://doi.org/10.5194/adgeo-22-3-2009

Garreaud, R. D., Vuille, M., Compagnucci, R., & Marengo, J. (2009). Present-day South American climate. *Palaeogeography, Palaeoclimatology, Palaeoecology*, *281*(3–4), 180–195. https://doi.org/10.1016/j.palaeo.2007.10.032

Gizaw, M. S., Gan, T. Y., Yang, Y., & Gan, K. E. (2021). Changes to the 1979–2013 summer Convective Available Potential Energy (CAPE) and extreme precipitation over North America. *Physics and Chemistry of the Earth*, *123*(July), 103047. https://doi.org/10.1016/j.pce.2021.103047

Grimm, A. M., Barros, V. R., & Doyle, M. E. (2000). Climate variability in southern South

America associated with El Nino and La Nina events. *Journal of Climate*, *13*(1), 35–58. https://doi.org/10.1175/1520-0442(2000)013<0035:CVISSA>2.0.CO;2

Hawkins, E., & Sutton, R. (2009). The potential to narrow uncertainty in regional climate predictions. *Bulletin of the American Meteorological Society*, *90*(8), 1095–1107. https://doi.org/10.1175/2009BAMS2607.1

Hersbach, H., Bell, B., Berrisford, P., Hirahara, S., Horányi, A., Muñoz-Sabater, J., Nicolas, J., Peubey, C., Radu, R., Schepers, D., Simmons, A., Soci, C., Abdalla, S., Abellan, X., Balsamo, G., Bechtold, P., Biavati, G., Bidlot, J., Bonavita, M., De Chiara, G., Dahlgren, P., Dee, D., Diamantakis, M., Dragani, R., Flemming, J., Forbes, R., Fuentes, M., Geer, A., Haimberger, L., Healy, S., Hogan, R. J., Hólm, E., Janisková, M., Keeley, S., Laloyaux, P., Lopez, P., Lupu, C., Radnoti, G., de Rosnay, P., Rozum, I., Vamborg, F., Villaume, S., & Thépaut, J.-N. (2020). The ERA5 global reanalysis. *Quarterly Journal of the Royal Meteorological Society*, *146*(730), 1999–2049. https://doi.org/10.1002/qj.3803

Holton, J. R., & Hakim, G. J. (2013). Mesoscale Circulations. In *An Introduction to Dynamic Meteorology*. https://doi.org/10.1016/b978-0-12-384866-6.00009-x

Hurrell, J. W., Holland, M. M., Gent, P. R., Ghan, S., Kay, J. E., Kushner, P. J., Lamarque, J.-F., Large, W. G., Lawrence, D., Lindsay, K., Lipscomb, W. H., Long, M. C., Mahowald, N., Marsh, D. R., Neale, R. B., Rasch, P., Vavrus, S., Vertenstein, M., Bader, D., Collins, W. D., Hack, J. J., Kiehl, J., & Marshall, S. (2013). The community earth system model: A framework for collaborative research. *Bulletin of the American Meteorological Society*, *94*(9), 1339–1360. https://doi.org/10.1175/BAMS-D-12-00121.1

Insel, N., Poulsen, C. J., & Ehlers, T. A. (2010). Influence of the Andes Mountains on South American moisture transport, convection, and precipitation. *Climate Dynamics*, *35*(7),

1477–1492. https://doi.org/10.1007/s00382-009-0637-1

IPCC, 2021: Climate Change 2021: The Physical Science Basis. Contribution of Working Group I to the Sixth Assessment Report of the Intergovernmental Panel on Climate Change[Masson-Delmotte, V., P. Zhai, A. Pirani, S.L. Connors, C. Péan, S. Berger, N. Caud, Y. Chen, L. Goldfarb, M.I. Gomis, M. Huang, K. Leitzell, E. Lonnoy, J.B.R. Matthews, T.K. Maycock, T. Waterfield, O. Yelekçi, R. Yu, and B. Zhou (eds.)]. Cambridge University Press, Cambridge, United Kingdom and New York, NY, USA, In press, doi:10.1017/9781009157896.

IPCC, 2022: Climate Change 2022: Impacts, Adaptation, and Vulnerability. Contribution of Working Group II to the Sixth Assessment Report of the Intergovernmental Panel on Climate Change [H.-O. Pörtner, D.C. Roberts, M. Tignor, E.S. Poloczanska, K. Mintenbeck, A. Alegría, M. Craig, S. Langsdorf, S. Löschke, V. Möller, A. Okem, B. Rama (eds.)]. Cambridge University Press. Cambridge University Press, Cambridge, UK and New York, NY, USA, 3056 pp., doi:10.1017/9781009325844.

Joetzjer, E., Douville, H., Delire, C., & Ciais, P. (2013). Present-day and future Amazonian precipitation in global climate models: CMIP5 versus CMIP3. *Climate Dynamics*, *41*(11–12), 2921–2936. https://doi.org/10.1007/s00382-012-1644-1

Klemp, J. B. (1987). Dynamics of tornadic thunderstorms. Annual review of fluid mechanics, 19(1), 369-402.

Lenters, J. D., & Cook, K. H. (1995). Simulation and Diagnosis of the Regional Summertime Precipitation Climatology of South America, *Journal of Climate*, *8*(12), 2988-3005. doi: https://doi.org/10.1175/1520-0442(1995)008<2988:SADOTR>2.0.CO;2

Lepore, C., Abernathey, R., Henderson, N., Allen, J. T., & Tippett, M. K. (2021). Future Global

Convective Environments in CMIP6 Models. *Earth's Future*, *9*(12), 1–21. https://doi.org/10.1029/2021EF002277

Li, F., Chavas, D. R., Reed, K. A., & Dawson, D. T. (2020). Climatology of severe local storm environments and synoptic-scale features over North America in ERA5 reanalysis and CAM6 simulation. *Journal of Climate*, *33*(19), 8339–8365. https://doi.org/10.1175/JCLI-D-19-0986.1

Lilly, D. K. (1979). The dynamical structure and evolution of thunderstorms and squall lines. Annual Review of Earth and Planetary Sciences, 7(1), 117-161.

Malhi, Y., Aragão, L. E. O. C., Galbraith, D., Huntingford, C., Fisher, R., Zelazowski, P., Sitch, S., McSweeney, C., & Meir, P. (2009). Exploring the likelihood and mechanism of a climate-change-induced dieback of the Amazon rainforest. *Proceedings of the National Academy of Sciences of the United States of America*, *106*(49), 20610–20615. https://doi.org/10.1073/pnas.0804619106

Malhi, Y., Roberts, J. T., Betts, R. A., Killeen, T. J., Li, W., & Nobre, C. A. (2008). Climate change, deforestation, and the fate of the Amazon. *Science*, *319*(5860), 169–172. https://doi.org/10.1126/science.1146961

Milinski, S., Maher, N., & Olonscheck, D. (2020). How large does a large ensemble need to be? *Earth System Dynamics*, *11*(4), 885–901. https://doi.org/10.5194/esd-11-885-2020

Montini, T. L., Jones, C., & Carvalho, L. M. V. (2019). The South American Low-Level Jet: A New Climatology, Variability, and Changes. *Journal of Geophysical Research: Atmospheres*, *124*(3), 1200–1218. https://doi.org/10.1029/2018JD029634

Qin, J., & Robinson, W. A. (1993). On the Rossby Wave Source and the Steady Linear Response to Tropical Forcing, *Journal of Atmospheric Sciences*, *50*(12), 1819-1823. doi:

https://doi.org/10.1175/1520-0469(1993)050<1819:OTRWSA>2.0.CO;2

Rasmussen, E. N., & Blanchard, D. O. (1998). A baseline climatology of sounding-derived supercell and tornado forecast parameters. *Weather and Forecasting*, *13*(4), 1148–1164. https://doi.org/10.1175/1520-0434(1998)013<1148:ABCOSD>2.0.CO;2

Rasmussen, K. L., Chaplin, M. M., Zuluaga, M. D., & Houze, R. A. (2016). Contribution of extreme convective storms to rainfall in South America. *Journal of Hydrometeorology*, *17*(1), 353–367. https://doi.org/10.1175/JHM-D-15-0067.1

Rasmussen, K. L., & Houze, R. A. (2011). Orogenic convection in subtropical South America as seen by the TRMM satellite. *Monthly Weather Review*, *139*(8), 2399–2420. https://doi.org/10.1175/MWR-D-10-05006.1

Rasmussen, K. L., & Houze, R. A. (2016). Convective initiation near the Andes in subtropical South America. *Monthly Weather Review*, *144*(6), 2351–2374. https://doi.org/10.1175/MWR-D-15-0058.1

Rasmussen, K. L., Prein, A. F., Rasmussen, R. M., Ikeda, K., & Liu, C. (2020). Changes in the convective population and thermodynamic environments in convection-permitting regional climate simulations over the United States. *Climate Dynamics*, *55*(1–2), 383–408. https://doi.org/10.1007/s00382-017-4000-7

Rasmussen, K. L., Zuluaga, M. D., & Houze, R. A. (2014). Severe convection and lightning in subtropical South America. *Geophysical Research Letters*, *41*(20), 7359–7366. https://doi.org/10.1002/2014GL061767

Reboita, M. S., Kuki, C. A. C., Marrafon, V. H., de Souza, C. A., Ferreira, G. W. S., Teodoro, T., & Lima, J. W. M. (2022). South America climate change revealed through climate indices projected by GCMs and Eta-RCM ensembles. *Climate Dynamics*, *58*(1–2), 459–

485. https://doi.org/10.1007/s00382-021-05918-2

Ribeiro, B. Z., & Bosart, L. F. (2018). Elevated Mixed Layers and Associated Severe Thunderstorm Environments in South and North America, *Monthly Weather Review, 146*(1), 3-28. doi: https://doi.org/10.1175/MWR-D-17-0121.1

Riemann-Campe, K., Fraedrich, K., & Lunkeit, F. (2009). Global climatology of Convective Available Potential Energy (CAPE) and Convective Inhibition (CIN) in ERA-40 reanalysis. *Atmospheric Research*, *93*(1–3), 534–545. https://doi.org/10.1016/j.atmosres.2008.09.037

Rochette, S. M., Moore, J. T., & Louis, S. (1999). The Importance of Parcel Choice in Elevated CAPE Computations. *National Weather Digest*, *23*(4), 20-32.

Rodgers, K. B., Lee, S. S., Rosenbloom, N., Timmermann, A., Danabasoglu, G., Deser, C., Edwards, J., Kim, J. E., Simpson, I. R., Stein, K., Stuecker, M. F., Yamaguchi, R., Bódai, T., Chung, E. S., Huang, L., Kim, W. M., Lamarque, J. F., Lombardozzi, D. L., Wieder, W. R., & Yeager, S. G. (2021). Ubiquity of human-induced changes in climate variability. *Earth System Dynamics*, *12*(4), 1393–1411. https://doi.org/10.5194/esd-12-1393-2021

Romatschke, U., & Houze, R. A. (2010). Extreme summer convection in South America. *Journal of Climate*, *23*(14), 3761–3791. https://doi.org/10.1175/2010JCLI3465.1

Rotunno, R., Klemp, J. B., & Weisman, M. L. (1988). A Theory for Strong, Long-Lived Squall Lines, *Journal of Atmospheric Sciences*, *45*(3), 463-485. https://doi.org/10.1175/1520-0469(1988)045<0463:ATFSLL>2.0.CO;2

Salio, P., Nicolini, M., & Zipser, E. J. (2007). Mesoscale convective systems over southeastern South America and their relationship with the South American low-level jet. *Monthly*

Weather Review, *135*(4), 1290–1309. https://doi.org/10.1175/MWR3305.1

Sardeshmukh, P. D., & Hoskins, B. J. (1988). The Generation of Global Rotational Flow by Steady Idealized Tropical Divergence, *Journal of Atmospheric Sciences*, *45*(7), 1228-1251. https://doi.org/10.1175/1520-0469(1988)045<1228:TGOGRF>2.0.CO;2

Schumacher, R. S., Hence, D. A., Nesbitt, S. W., Trapp, R. J., Kosiba, K. A., Wurman, J., Salio, P., Rugna, M., Varble, A. C., & Kelly, N. R. (2021). Convective-Storm Environments in Subtropical South America from High-Frequency Soundings during RELAMPAGO-CACTI, Monthly Weather Review, 149(5), 1439-1458. https://doi.org/10.1175/MWR-D-20-0293.1

Seager, R., Henderson, N., & Cane, M. (2022). Persistent Discrepancies between Observed and Modeled Trends in the Tropical Pacific Ocean. *Journal of Climate*, *35*(14), 4571–4584. https://doi.org/10.1175/JCLI-D-21-0648.1

Seeley, J. T., & Romps, D. M. (2015). The effect of global warming on severe thunderstorms in the United States. *Journal of Climate*, *28*(6), 2443–2458. https://doi.org/10.1175/JCLI-D-14-00382.1

Simpson, I. R., Bacmeister, J., Neale, R. B., Hannay, C., Gettelman, A., Garcia, R. R., Lauritzen, P. H., Marsh, D. R., Mills, M. J., Medeiros, B., & Richter, J. H. (2020). An Evaluation of the Large-Scale Atmospheric Circulation and Its Variability in CESM2 and Other CMIP Models. *Journal of Geophysical Research: Atmospheres*, *125*(13), 1–42. https://doi.org/10.1029/2020JD032835

Taszarek, M., Allen, J. T., Marchio, M., & Brooks, H. E. (2021). Global climatology and trends in convective environments from ERA5 and rawinsonde data. *Npj Climate and Atmospheric Science*, *4*(1), 1–11. https://doi.org/10.1038/s41612-021-00190-x

Tippett, M. K., Allen, J. T., Gensini, V. A., & Brooks, H. E. (2015). Climate and Hazardous Convective Weather. *Current Climate Change Reports*, *1*(2), 60–73. https://doi.org/10.1007/s40641-015-0006-6

Trapp, R. J., Diffenbaugh, N. S., Brooks, H. E., Baldwin, M. E., Robinson, E. D., & Pal, J. S. (2007). Changes in severe thunderstorm environment frequency during the 21st century caused by anthropogenically enhanced global radiative forcing. *Proceedings of the National Academy of Sciences of the United States of America*, *104*(50), 19719–19723. https://doi.org/10.1073/pnas.0705494104

Velasco, I., and Fritsch, J. M. (1987). Mesoscale convective complexes in the Americas, *Journal of Geophysical. Research, 92*(D8), 9591– 9613, doi:10.1029/JD092iD08p09591.

Vera, C., Baez, J., Douglas, M., Emmanuel, C. B., Marengo, J., Meitin, J., Nicolini, M., Nogues-Paegle, J., Paegle, J., Penalba, O., Salio, P., Saulo, C., Silva Dias, M. A., Dias, P. S., & Zipser, E. (2006). The South American Low-Level Jet Experiment, *Bulletin of the American Meteorological Society, 87*(1), 63-78. https://doi.org/10.1175/BAMS-87-1-63

Virji, H. (1981). A Preliminary Study of Summertime Tropospheric Circulation Patterns over South America Estimated from Cloud Winds, *Monthly Weather Review, 109*(3), 599-610. doi: https://doi.org/10.1175/1520-0493(1981)109<0599:APSOST>2.0.CO;2

Wang, J., Chagnon, F. J. F., Williams, E. R., Betts, A. K., Renno, N. O., Machado, L. A. T., Bisht, G., Knox, R., & Bras, R. L. (2009). Impact of deforestation in the Amazon basin on cloud climatology. *Proceedings of the National Academy of Sciences of the United States of America*, *106*(10), 3670–3674. https://doi.org/10.1073/pnas.0810156106

Wei, Y., Yu, H., Huang, J., He, Y., Yang, B., Guan, X., & Liu, X. (2018). Comparison of the Pacific Decadal Oscillation in climate model simulations and observations. *International*

Journal of Climatology, *38*(November 2017), e99–e118. https://doi.org/10.1002/joc.5355

Weisman, M. L., & Rotunno, R. (2000). The use of vertical wind shear versus helicity in interpreting supercell dynamics. *Journal of the Atmospheric Sciences*, *57*(9), 1452–1472. https://doi.org/10.1175/1520-0469(2000)057<1452:TUOVWS>2.0.CO;2

Yin, L., Fu, R., Shevliakova, E., & Dickinson, R. E. (2013). How well can CMIP5 simulate precipitation and its controlling processes over tropical South America? *Climate Dynamics*, *41*(11–12), 3127–3143. https://doi.org/10.1007/s00382-012-1582-y

Zipser, E. J., Cecil, D. J., Liu, C., Nesbitt, S. W., & Yorty, D. P. (2006). Where are the most: Intense thunderstorms on Earth? *Bulletin of the American Meteorological Society*, *87*(8), 1057–1071. https://doi.org/10.1175/BAMS-87-8-1057